20. Стрельникова Е. А. Гиперсингулярные интегральные уравнения в двумерных краевых задачах для уравнения Лапласа и уравнений Ламе. *Доп. НАН України*. 2001. № 3. С. 27–31.
21. Кантор Б. Я., Стрельникова Е. А. Гиперсингулярные интегральные уравнения в задачах механики сплошной среды. Харьков: Новое слово, 2005. 252 с.
22. Gnitko V., Naumemko Y., Strelnikova E. Low frequency sloshing analysis of cylindrical containers with flat and conical baffles. *Intern. J. Appl. Mech. and Eng*. 2017. Vol. 22. Iss. 4. P. 867–881. https://doi.org/10.1515/ijame-2017-0056.
23. Пэрис П., Эрдоган Ф. Критерии усталостного распространения трещин. *Техн. механика*. Сер. Д. 1987. № 4. С. 60–68.
24. Стрельникова Е. А., Сирота И. Г., Линник А. В., Калембет Л. А, Зархина В. Н., Зайденварг О. Л. Вероятностная оценка долговечности вала гидротурбины при наличии трещин. *Пробл. машиностроения*. 2017. Т. 20. № 1. С. 28–35. https://doi.org/10.15407/pmach2017.01.028
25. Берендеев Н. Н. Применение системы ANSYS к оценке усталостной долговечности. Нижний Новгород: Нижегород. ун-т им. Н. И. Лобачевского, 2006. 84 с.

DOI: https://doi.org/10.15407/pmach2020.01.038

UDC 539.3

METHOD TO STUDY THE CREEP OF COMPLEX-SHAPED FUNCTIONALLY-GRADED BODIES

Serhii M. Sklepus
snsklepus@ukr.net
ORCID: 0000-0002-4119-4310

A. Podgorny Institute
of Mechanical Engineering
Problems of NASU,
2/10, Pozharskyi St., Kharkiv,
61046, Ukraine

The creep problem of complex-shaped functionally-graded bodies of revolution is considered. For the variational statement of the problem, the Lagrange functional is used, defined at kinematically possible displacement rates. A numerical-analytical method is developed for solving a non-linear initial-boundary creep problem. It is based on the combined use of the R-functions, Ritz and Runge-Kutta-Merson methods. The advantages of the proposed method include: exact consideration of the geometric information about the boundary-value problem at the analytical level, without any approximation thereof; representation of an approximate solution to the problem in an analytical form; exact satisfaction of boundary conditions; automatic time step selection. Solved are the problems of creep both for a hollow straight cylinder and a complex-shaped body of revolution (a cylinder with a rectangular cut-out on the outer surface), both cylinders being loaded with a constant inner pressure, made of the functionally graded material (FGM) based on SiC particle-reinforced aluminium. The creep of the material is described by Norton' law. Both Young's modulus and creep characteristics of the material depend on the volume part of the reinforcing material. Both ends of the cylinder are free of external load, and are fixed in such a way that the radial displacements are equal to zero. A corresponding partial solution structure is constructed that satisfies the boundary conditions for displacement rates. The calculations were performed for cylinders of two different composite materials: a material with a uniform distribution of SiC particles and an FGM with a difference in the volume content of reinforcing particles along the radius, with the average volumetric content of reinforcing SiC particles in the two cases being the same. The influence of both the gradient properties of the material and geometric shape on the stress-strain state (SSS) under creep conditions was investigated. The presence of a rectangular cut-out on the outer surface of a cylinder in all cases leads to an increase in displacements and stresses. Moreover, the degree of influence of the geometric shape on the SSS during creep substantially depends on the gradient properties of the material. For a cut-out cylinder made of the material with a uniform distribution of SiC particles, there is a significant increase in displacements and stresses after 100 hours of creep compared with a straight cylinder. For bodies of revolution made of a functionally graded material, the cut-out effect on the SSS is less pronounced.

Keywords: *functionally graded material, body of revolution, creep, R-functions method.*

Introduction

Axisymmetric bodies, as structural elements, are used in power engineering, space engineering, chemical industry, and other branches. These are pressure vessels (hydraulic cylinders, pipes, boilers, fuel tanks, etc.), gas turbines, accumulator shells, cylinders for the aerospace industry, nuclear reactors, pipelines of nuclear reactors. They can be made of both uniform and composite materials, which include functionally graded materials (FGM). The composition and structure of FGMs change according to some law, which leads to corresponding changes in both mechanical and physical properties. This allows them to be used in structural elements operating in extreme conditions with significant thermo-mechanical loads. The theory and methods of calculating the creep of structural elements, in particular FGM cylinders and bodies of revolution are being intensively developed. Most often, bodies of a canonical geometric shape are considered: straight hollow cylinders, spheres, cones [1–6]. In this case, various assumptions are often introduced both to simplify the initial-boundary creep problem and obtain an analytical solution. If the body of revolution has a complex geometric shape, then the creep problem fails to be solved analytically. In this case, to solve the boundary-value problem, it is necessary to use numerical methods that allow finding an approximate solution in complex-shaped areas, for example, the finite element method [7, 8], the R-functions method [9,10], the immersion method [11, 12], and others. Unlike other methods, the R-functions method allows us both to accurately take into account the geometric information about the boundary-value problem and to present an approximate solution in the form of a formula – a solution structure that exactly satisfies all boundary conditions (general structure) or their part (partial structure).

The aim of the article is to develop a numerical-analytical method for solving the creep problems of complex-shaped axisymmetrically-loaded functionally-graded bodies of revolution, as well as to study both the influence of gradient material properties and geometric shapes on the SSS of bodies of revolution under creep conditions.

Problem Formulation. Solution method

Let us consider an axisymmetrically loaded FGM body of revolution with an arbitrary shape of meridional section in the cylindrical coordinate system $Or\varphi z$. The Oz axis coincides with the axis of rotation. The elastic and creep characteristics monotonically vary in the radial direction. The components of the total strain rate tensor $\dot{\varepsilon}_{kl}(r,z,t)$ can be represented as the sum of the rates of both the elastic strains $\dot{\varepsilon}^e_{kl}(r,z,t)$ and creep strains $\dot{p}_{kl}(r,z,t)$

$$\dot{\varepsilon}_{rr}=\dot{\varepsilon}^e_{rr}+\dot{p}_{rr};\ \dot{\varepsilon}_{zz}=\dot{\varepsilon}^e_{zz}+\dot{p}_{zz};\ \dot{\varepsilon}_{\varphi\varphi}=\dot{\varepsilon}^e_{\varphi\varphi}+\dot{p}_{\varphi\varphi};\ \dot{\varepsilon}_{rz}=\dot{\varepsilon}^e_{rz}+\dot{p}_{rz}.$$

Hereinafter, the dot above the symbols means the total time derivative *t*.

The main unknowns of a creep problem at any point of the body at time instants $t>0$ can be found from solving the time-dependent Cauchy problem for the system of ordinary differential equations

$$\left.\begin{gathered}
\frac{du_r}{dt}=\dot{u}_r;\quad \frac{du_z}{dt}=\dot{u}_z;\\
\frac{d\varepsilon_{rr}}{dt}=\dot{u}_{r,r};\ \frac{d\varepsilon_{zz}}{dt}=\dot{u}_{z,z};\ \frac{d\varepsilon_{\varphi\varphi}}{dt}=\dot{u}_r r^{-1};\ \frac{d\gamma_{rz}}{dt}=2\frac{d\varepsilon_{rz}}{dt}=\dot{u}_{r,z}+\dot{u}_{z,r};\\
\frac{d\sigma_{rr}}{dt}=\lambda_1(r)(\dot{\varepsilon}_{rr}-\dot{p}_{rr})+\lambda(r)(\dot{\varepsilon}_{zz}+\dot{\varepsilon}_{\varphi\varphi}-\dot{p}_{zz}-\dot{p}_{\varphi\varphi});\\
\frac{d\sigma_{zz}}{dt}=\lambda_1(r)(\dot{\varepsilon}_{zz}-\dot{p}_{zz})+\lambda(r)(\dot{\varepsilon}_{rr}+\dot{\varepsilon}_{\varphi\varphi}-\dot{p}_{rr}-\dot{p}_{\varphi\varphi});\\
\frac{d\sigma_{\varphi\varphi}}{dt}=\lambda_1(r)(\dot{\varepsilon}_{\varphi\varphi}-\dot{p}_{\varphi\varphi})+\lambda(r)(\dot{\varepsilon}_{rr}+\dot{\varepsilon}_{zz}-\dot{p}_{rr}-\dot{p}_{zz});\\
\frac{d\sigma_{rz}}{dt}=G(r)(\dot{\gamma}_{rz}-2\dot{p}_{rz});\\
\frac{dp_{rr}}{dt}=\dot{p}_{rr};\ \frac{dp_{zz}}{dt}=\dot{p}_{zz};\ \frac{dp_{\varphi\varphi}}{dt}=\dot{p}_{\varphi\varphi};\ \frac{dp_{rz}}{dt}=\dot{p}_{rz}.
\end{gathered}\right\}\qquad(1)$$

Here, $u_r(r,z,t)$, $u_z(r,z,t)$ are the displacements along the axes Or and Oz, respectively; $\varepsilon_{rr}, \varepsilon_{zz}, \varepsilon_{\varphi\varphi}, \varepsilon_{rz}$ are the components of the total strain tensor; p_{rr}, p_{zz}, $p_{\varphi\varphi}$, p_{rz} are the components of the creep strain tensor; $\sigma_{rr}, \sigma_{zz}, \sigma_{\varphi\varphi}, \sigma_{rz}$ are the components of the stress tensor; $\lambda(r)=\dfrac{E(r)\nu(r)}{(1-2\nu(r))(1+\nu(r))}$; $\lambda_1(r)=\lambda(r)+2G(r)$; $G(r)=\dfrac{E(r)}{2(1+\nu(r))}$, where $E(r), \nu(r)$ are Young's modulus and Poisson's ratio of the material.

At the initial time instant, the creep strains $p_{rr}=p_{zz}=p_{\varphi\varphi}=2p_{rz}=0$. The initial conditions for the remaining unknown functions are found from the solution to the elastic deformation problem.

The right-hand sides of the equations of system (1) depend on the form of the constitutive equations for creep strain rates. Suppose that the creep of a material can be described using Norton's law [5]. In this case, the constitutive equations of creep will have the form

$$\dot{p}_{rr}=\frac{3}{2}A(r)\sigma_i^{n(r)-1}\left(\sigma_{rr}-\frac{1}{3}I_1\right);\ \dot{p}_{zz}=\frac{3}{2}A(r)\sigma_i^{n(r)-1}\left(\sigma_{zz}-\frac{1}{3}I_1\right);$$

$$\dot{p}_{\varphi\varphi}=\frac{3}{2}A(r)\sigma_i^{n(r)-1}\left(\sigma_{\varphi\varphi}-\frac{1}{3}I_1\right);\ \dot{p}_{rz}=\frac{3}{2}A(r)\sigma_i^{n(r)-1}\sigma_{rz}; \qquad (2)$$

where $\sigma_i=\sqrt{\sigma_{rr}^2+\sigma_{zz}^2+\sigma_{\varphi\varphi}^2-\sigma_{rr}\sigma_{zz}-\sigma_{rr}\sigma_{\varphi\varphi}-\sigma_{zz}\sigma_{\varphi\varphi}+3\sigma_{rz}^2}$ is the stress intensity; $I_1=\sigma_{rr}+\sigma_{zz}+\sigma_{\varphi\varphi}$; $A(r)$, $n(r)$ are the FGM creep characteristics.

We will solve the initial problem for the system of equations (1) by the Runge-Kutta-Merson (RKM) method with automatic time step selection. The right-hand sides of equations (1) at the time instants corresponding to the RKM scheme are found by solving the variational problem for the Lagrange functional [13]

$$\Lambda(\dot{\mathbf{U}})=0{,}5\iint_\Omega\left[\lambda_1(r)\left(\dot{u}_{r,r}^2+\dot{u}_{z,z}^2+r^{-2}\dot{u}_r^2\right)+G(r)\left(\dot{u}_{r,z}+\dot{u}_{z,r}\right)^2+2\lambda(r)\left(\dot{u}_{r,r}\dot{u}_{z,z}+r^{-1}\dot{u}_r\left(\dot{u}_{r,r}+\dot{u}_{z,r}\right)\right)\right]r\,dr\,dz-$$

$$-\iint_\Omega\left[\dot{u}_{r,r}\dot{N}_{rr}^c+\dot{u}_{z,z}\dot{N}_{zz}^c+\dot{u}_r r^{-1}\dot{N}_{\varphi\varphi}^c+\dot{N}_{rz}^c\left(\dot{u}_{r,z}+\dot{u}_{z,r}\right)\right]r\,dr\,dz-\int_{\partial\Omega_p}\left(\dot{P}_n\dot{u}_n+\dot{P}_\tau\dot{u}_\tau\right)d\partial\Omega. \qquad (3)$$

Here, $\dot{\mathbf{U}}$ is the vector of kinematically possible deplacement rates: $\dot{\mathbf{U}}=(\dot{u}_r(r,z,t),\dot{u}_z(r,z,t))$; Ω is the meridional section of the body; $\partial\Omega_p$ is part of the boundary where external forces are applied; $\dot{P}_n$, $\dot{P}_\tau$ are the rates of the normal and tangential components of external boundary forces; n, τ are the external normal and tangent to the boundary $\partial\Omega$; $\dot{u}_n=\dot{u}_r n_r+\dot{u}_z n_z$, $\dot{u}_\tau=\dot{u}_z n_r\quad \dot{u}_r n_z$; n_r, n_z are the direction cosines of the normal n. The rates of "fictitious forces" caused by creep are calculated by the formulas

$$\dot{N}_{rr}^c=\left[\lambda_1(r)\dot{p}_{rr}+\lambda(r)\left(\dot{p}_{zz}+\dot{p}\quad\right)\right],\ \dot{N}_{zz}^c=\left[\lambda_1(r)\dot{p}_{zz}+\lambda(r)\left(\dot{p}_{rr}+\dot{p}\quad\right)\right],$$

$$\dot{N}^c\ =\left[\lambda_1(r)\dot{p}\quad+\lambda(r)\left(\dot{p}_{rr}+\dot{p}_{zz}\right)\right],\ N_{rz}^c=2G(r)\dot{p}_{rz}.$$

The creep strain rates in functional (3) are assumed to be known, and therefore they do not vary.

We will solve the variational problems for functional (3) by the Ritz method in combination with the R-functions method [9, 10].

The advantages of the proposed method include: accurate consideration of geometric information about a boundary value problem at the analytical level, without any approximation thereof; presentation of an approximate solution to the problem in an analytical form; exact satisfaction of boundary conditions; automatic time step selection.

Numerical Studies

Let us consider the creep of both a straight hollow cylinder and a complex-shaped body of revolution (a cylinder with a rectangular cut-out on the outer surface) formed by rotating a plane figure around the Oz axis (Fig. 1) and made of the FGM based on SiC-reinforced aluminum. Both the cylinder and the body of revolution are loaded by the internal pressure with intensity P_{in}=50 MPa. Geometrical dimensions are: a=0.01 m, b=0.02 m, c=0.018, d=0.02 m, length l=0.1 m.

Numerical Studies

Let us consider the creep of both a straight hollow cylinder and a complex-shaped body of revolution (a cylinder with a rectangular cut-out on the outer surface) formed by rotating a plane figure around the Oz axis (Fig. 1) and made of the FGM based on SiC-reinforced aluminum. Both the cylinder and the body of revolution are loaded by the internal pressure with intensity P_{in}=50 MPa. Geometrical dimensions are: a=0.01 m, b=0.02 m, c=0.018, d=0.02 m, length l=0.1 m.

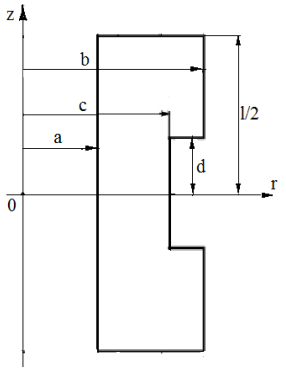

Fig. 1. The plane region forming the body of revolution

The content of ceramic SiC particles varies linearly along the radius, and the volume fraction of ceramics (%) with a given radius obeys the law [14]

$$V(r)=V_{\max}-\left(\frac{r-a}{b-a}\right)(V_{\max}-V_{\min})$$

where $V_{\max}$ and $V_{\min}$ are the maximum and minimum contents of reinforcing SiC particles both on the inner and outer surfaces, respectively.

Young's modulus [MPa] of the FGM depends on the volume part of the reinforcing material, and approximately obeys the linear law [15]

$$E(r)=6.9\cdot10^{4}+1.33\cdot10^{3}V(r).$$

Poisson's ratio ν=0.3.

The FGM creep characteristics depend on $V(r)$, and vary along the radial coordinate as follows [16]:

$$A(r)=A_0\left[\frac{V(r)}{V_0}\right]^{\phi},\ n(r)=n_0\left[\frac{V(r)}{V_0}\right]^{-\phi},$$

where $A_0=9.972\cdot10^{-13}$ MPa$^{-n_0}$h^{-1}; $n_0=3.75$; $\phi=0.7$; V_0 is the average volumetric content of ceramics in the cylinder.

Both ends of the cylinder $z=\pm l/2$ are free of external load, and are fixed in such a way that the radial displacements u_r are equal to zero. In this case, the boundary conditions of the creep problem will have the form

$$\dot{u}_r=0,\ \dot{\sigma}_{zz}=0 \text{ at } z=\pm l/2;$$

$$\dot{\sigma}_{rr}=-\dot{P}_{in}=0,\ \dot{\sigma}_{zr}=0 \text{ at } r=a;$$

$$\dot{\sigma}_n=\dot{\sigma}_\tau=0 \text{ for points on the outer surface.}$$

Here, σ_n, σ_τ are the normal and tangential stresses: $\sigma_n=\sigma_{rr}n_r^2+2\sigma_{rz}n_rn_z+\sigma_{zz}n_z^2$, $\dot{\sigma}_\tau=(\sigma_{zz}-\sigma_{rr})n_rn_z+\sigma_{rz}(n_r^2-n_z^2)$.

The corresponding partial solution structure satisfying the boundary conditions for displacement rates can be written as follows:

$$\dot{u}_r=\omega_1\Phi_1,\ \dot{u}_z=z\Phi_2, \tag{4}$$

where Φ_1,Φ_2 are the indefinite components of the solution structure; $\omega_1=\frac{1}{l}\left(\frac{l^2}{4}-z^2\right)\geq0$ is the strip Ω_1 enclosed between the lines $z=-l/2$ and $z=l/2$ ($\omega_1=0$, $\omega_{1,n}=-1$ on the border $\partial\Omega_1$, $\omega_1>0$ inside the strip).

In the numerical implementation, the indefinite components Φ_1, Φ_2 are represented as finite series of the form

$$\Phi_1(r,z,t)=\sum_{n=1}^{N_1}C_n^{(1)}(t)f_n^{(1)}(r,z);\ \ \Phi_2(r,z,t)=\sum_{n=1}^{N_2}C_n^{(2)}(t)f_n^{(2)}(r,z),$$

where $C_n^{(1)}(t)$, $C_n^{(2)}(t)$ are the indefinite coefficients, which at each time step are found by the Ritz method; t is a certain fixed instant of time discretization of the RKM scheme or time discretization to produce compu-

tation results; $\{f_n^{(1)}\}$, $\{f_n^{(2)}\}$ are the systems of linearly independent functions, which are based on Schoenberg bicubic splines. Spline systems are built on a regular grid $K_r \times K_z$, where K_r, K_z are the numbers of discretization segments along the axes Or and Oz, respectively.

The equation of the boundary of the region shown in Fig. 1 can be written as

$$\omega(r,z) = (\omega_1 \wedge_0 \omega_2) \wedge_0 (\omega_3 \vee_0 \omega_4) = 0. \quad (5)$$

Here, $\omega_1, \omega_2, \omega_3, \omega_4$ are the supporting regions forming the region Ω: $\omega_1 = \frac{1}{l}\left(\frac{l^2}{4} - z^2\right)$, $\omega_2 = \frac{(r-a)(b-r)}{b-a}$, $\omega_3 = c - r$, $\omega_4 = \frac{1}{2d}\left(z^2 - d^2\right)$, $\wedge_0$, $\wedge_0$ denote the R-conjunction and the R-disjunction [9,10]:

$$f_1 \wedge_0 f_2 = f_1 + f_2 - \sqrt{f_1^2 + f_2^2}, \quad f_1 \vee_0 f_2 = f_1 + f_2 + \sqrt{f_1^2 + f_2^2}.$$

Since the structure of solution (4) satisfies only kinematic boundary conditions, the function $\omega = \omega(r,z)$ that describes the geometry of the region is not included therein. Equation (5) was used to spatially discretize the problem and to find the coordinates of the nodes of the integration grid. The spatial sampling parameters are the following: $K_r = 20$, $K_z = 20$ for a cut-out cylinder and $K_r = 10$, $K_z = 20$, for a straight cylinder. The specified calculation error in the RCM method is $\varepsilon = 10^{-3}$.

The calculations were performed for cylinders of two different composite materials (see the table): a material with a uniform distribution of SiC particles (I) and an FGM (II) with a difference in the volume content of reinforcing particles along the radius. The average volumetric content of SiC particles is the same in all cases.

The content of reinforcing particles in the material

Material	V_{max}, %	V_0, %	V_{min}, %
I	20	20	20
II	30	20	12

Some calculation results in the centers of the cylinders are presented in Figs. 2 to 6. The solid lines show the results of calculations for the straight cylinder, and the dashed lines, for the cut-out cylinder. Figs. 2 and 3 show the growth of radial displacements on the inner surface of the cylinders, where they are maximal.

Figs. 4 to 6 illustrate the time variation of the circumferential stresses on the inner and outer surfaces of the cylinders.

In the creep process, there is an increase in displacements and redistribution of stresses. The circumferential stresses at the initial instant of time are maximal on the inner surface. Then, due to creep, in the cylinder with a uniform distribution of the reinforcing material, stress relaxation occurs on the inner surface (Fig. 4), and stress increase, on the outer surface (Fig. 6, curve 1). The opposite picture is observed for FGM cylinders: stress increase occurs on the inner surface (Fig. 5), and stress relaxation, on the outer surface (Fig. 6, curve 2).

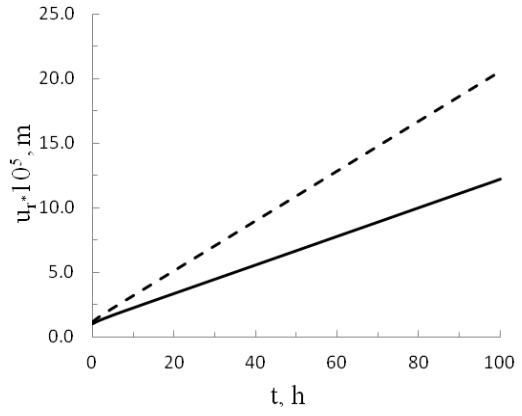

Fig. 2. The growth of the radial displacements on the inner surfaces of cylinders with uniform distribution of reinforcing particles

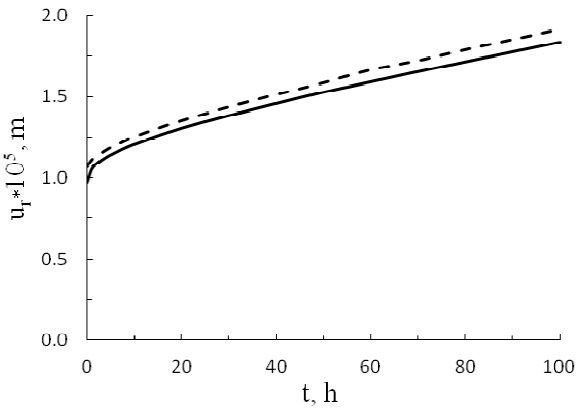

Fig. 3. The growth of the radial displacements on the inner surfaces of FGM cylinders

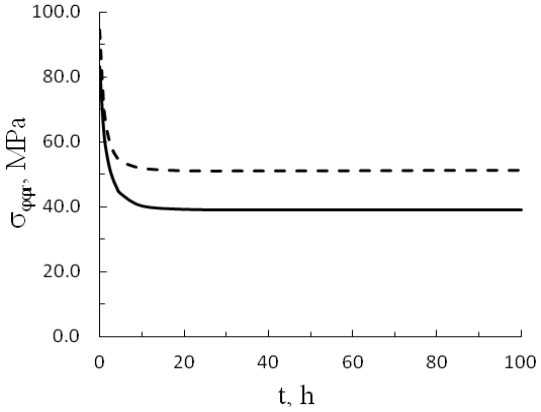

Fig. 4. The temporal variation for the circumferential stresses on the inner surfaces of the cylinders with a uniform distribution of reinforcing particles

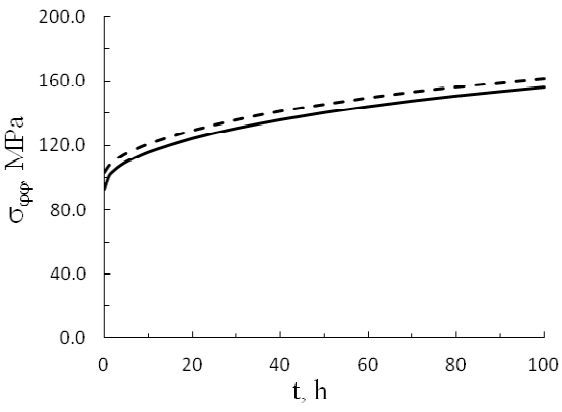

Fig. 5. The temporal variation for the circumferential stresses on the inner surfaces of FGM cylinders

The presence of a rectangular cut-out on the outer surface of the cylinder in all cases leads to an increase in displacements and stresses (Figs. 2–5), with the degree of influence of a geometric shape on the SSS during creep substantially depending on the properties of the material. Figs. 2, 5 show that for a cut-out cylinder made of a material with a uniform distribution of SiC particles, there is a significant increase in displacements ($\approx 70\,\%$) and stresses ($\approx 32\,\%$) after 100 h of creep, in comparison with a straight cylinder. For FGM bodies, the effect of the cut-out on the SSS is less pronounced (Fig. 3, 5). This is explained by the fact that the part of the cylinder where the content of reinforcing particles is minimal and creep is most intense was removed.

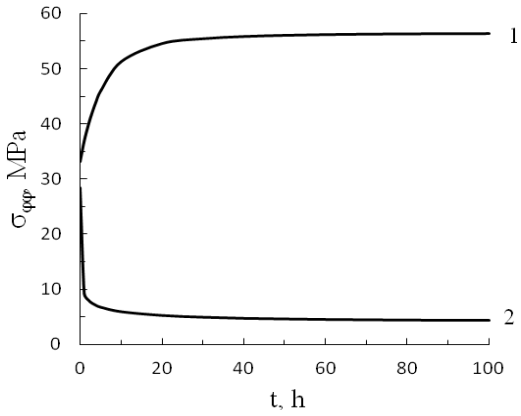

Fig. 6. The temporal variation for the circumferential stresses on the outer surfaces of straight cylinders: 1 – cylinder with a uniform distribution of reinforcing particles, 2 – FGM cylinder

Conclusions

The statement of the problem of creep of complex-shaped FGM bodies of revolution is presented. A numerical-analytical method is developed for solving the non-linear initial-boundary creep problem, which is based on the use of the R-functions, Ritz, and Rune-Kutta-Merson methods. Solved are the problems of creep both for a hollow straight cylinder and a complex-shaped body of revolution (a cylinder with a rectangular cut-out on the outer surface), both cylinders being loaded with a constant inner pressure, and made from the FGM based on SiC-reinforced aluminum. The influence of both gradient material properties and a geometric shape on the SSS under creep conditions is investigated.

References

1. Chen, J. J. (2007). Creep analysis for a functionally graded cylinder subjected to internal and external pressure. *J. Strain Analysis*, vol. 42, pp. 69–77. https://doi.org/10.1243/03093247JSA237.
2. Nejad, M. Z. & Kashkoli, M. D. (2014). Time-dependent thermo-creep analysis of rotating FGM thick-walled cylindrical pressure vessels under heat flux. *Int. J. Eng. Sci.*, vol. 82, pp. 222–237. https://doi.org/10.1016/j.ijengsci.2014.06.006.
3. Shrikant, K. V. (2012). Creep analysis of an isotropic functionally graded cylinder. *J. Advances in Sci. and Techn.*, vol. 3, no. 4, pp. 1–9.

4. Singh, T. & Gupta, V. K. (2011). Effect of anisotropy on steady state creep in functionally graded cylinder. *Composite Structures*, vol. 93, no. 2, pp. 747–758. https://doi.org/10.1016/j.compstruct.2010.08.005.
5. Chen, J. J., Yoon, K. B., & Tu, S. T. (2011). Creep behavior of pressurized tank composed of functionally graded materials. *J. Pressure Vessel Techn.*, vol. 133, pp. 69–77. https://doi.org/10.1115/1.4003455.
6. Kashkoli, M. D. & Nejad, M. Z. (2015). Time dependent thermo-elastic creep analysis of thick-walled spherical pressure vessels made of functionally graded materials. *J. Theoret. and Appl. Mech.*, vol. 53, no. 4, pp. 1053–1065. https://doi.org/10.15632/jtam-pl.53.4.1053.
7. Breslavskyi, D. V., Korytko, Yu. M., & Tatarinova, O. A. (2017). *Proektuvannia ta rozrobka skinchennoelementnoho prohramnoho zabezpechennia* [Design and development of finite element software]. Kharkiv: «Pidruchnyk NTU «KhPI», 232 p. (in Ukrainian).
8. Breslavsky, D., Kozlyuk, A., & Tatatarinova, O. (2018). Numerical simulation of two-dimensional problems of creep crack growth with material damage consideration. *Eastern-European Journal of Enterprise Technologies*, no. 2/7 (92), pp. 27–33. https://doi.org/10.15587/1729-4061.2018.119727.
9. Rvachev, V. L. (1982). *Teoriya R-funktsiy i nekotoryye yeye prilozheniya* [The R-functions theory and some of its applications]. Kiyev: Naukova Dumka, 552 p. (in Russian).
10. Rvachev, V. L. & Sinekop, N. S. (1990). *Metod R-funktsiy v zadachakh teorii uprugosti i plastichnosti* [The R-functions method in problems of the theory of elasticity and plasticity]. Kiyev: Naukova dumka, 216 p. (in Russian).
11. Rodichev, Y. M., Smetankina, N. V., Shupikov, O. M., & Ugrimov, S. V. (2018). Stress-strain assessment for laminated aircraft cockpit windows at static and dynamic loads. *Strength of Materials*, vol. 50, iss. 6, pp. 868–873. https://doi.org/10.1007/s11223-019-00033-4.
12. Smetankina, N. V. (2015). *Modeliuvannia kolyvan sharuvatykh tsylindrychnykh obolonok skladnoi formy pry udar-nomu navantazhenni* [Modeling of oscillations of layered cylindrical shells of complex shape at impact loading]. *Visn. Zaporiz. nats. un-tu. Fizyko-matematychni nauky – Bulletin of Zaporizhzhya National University. Physical and mathematical sciences*, no. 1, pp. 162–170 (in Ukrainian).
13. Zolochevsky, A., Sklepus, S., Galishin, A., Kühhorn, A., Kober, M. (2014). A comparison between the 3D and the Kirchhoff-Love solutions for cylinders under creep-damage conditions. *Techn. Mechanik*, vol. 34, no. 2, pp. 104–113.
14. Singh, S. B. & Ray, S. (2003). Creep analysis in an isotropic FGM rotating disc of Al–SiC composite. *J. Materials Proc. Techn.*, vol. 143–144, pp. 616-622. https://doi.org/10.1016/S0924-0136(03)00445-X.
15. Ogierman, W. & Kokot, G. (2013). Mean field homogenization in multi-scale modelling of composite materials. *J. Achievements in Materials Manufacturing Eng. (JAMME)*, vol. 61, iss. 2, pp. 343–348.
16. Singla, A., Gard, M., & Gupta, V. K. (2015). Steady state creep behaviour of functionally graded composite by using analytical method. *Intern. J. Computer Appl.*, no. 8, pp. 13–17.

Received 10 February 2020

Метод дослідження повзучості функціонально-градієнтних тіл складної форми

С. М. Склепус

Інститут проблем машинобудування ім. А. М. Підгорного НАН України,
61046, Україна, м. Харків, вул. Пожарського, 2/10

Розглянуто задачу повзучості тіл обертання складної форми із функціонально-градієнтних матеріалів. Для варіаційної постановки задачі використовується функціонал у формі Лагранжа, заданий на кінематично можливих швидкостях переміщень. Розроблено числово-аналітичний метод розв'язання нелінійної початково-крайової задачі повзучості, який базується на спільному застосуванні методів R-функцій, Рітца та Рунге-Кутта-Мерсона. До переваг запропонованого методу можна віднести: точне урахування геометричної інформації про крайову задачі на аналітичному рівні, без будь-якої її апроксимації, подання наближеного розв'язку задачі в аналітичному вигляді, автоматичний вибір часового кроку. Розв'язано задачі повзучості порожнистого циліндра і тіла обертання складної форми – циліндра з прямокутним вирізом на зовнішній поверхні, навантажених постійним внутрішнім тиском, виконаних із функціонально-градієнтного матеріалу на основі алюмінію, армованого частинками карбіду кремнію SiC. Повзучість матеріалу описується законом Нортона. Модуль Юнга і характеристики повзучості залежать від об'ємної частини армуючого матеріалу. Обидва кінці циліндра вільні від зовнішнього навантаження і закріплені таким чином, що радіальні переміщення дорівнюють нулю. Побудована відповідна часткова структура розв'язку, що задовольняє граничні умови для швидкостей переміщень. Розрахунки виконані для циліндрів з двох різних композиційних матеріалів – матеріалу з однорідним розподілом SiC-частинок і функціонально-градієнтного матеріалу з перепадом об'ємного вмісту армуючих частинок уздовж радіуса. При цьому середнє значення об'ємного вмісту армуючих SiC-частинок в двох випадках було однаковим. Досліджено вплив градієнтних властивостей матеріалу і геометричної форми на на-

пружено-деформований стан при повзучості. Наявність на зовнішній поверхні циліндра прямокутного вирізу призводить у всіх випадках до збільшення переміщень і напружень. При цьому ступінь впливу геометричної форми на напружено-деформований стан при повзучості істотно залежить від градієнтних властивостей матеріалу. Для циліндра з вирізом, виконаного з матеріалу з однорідним розподілом SiC-частинок, спостерігається значне зростання переміщень і напружень після 100 годин повзучості, в порівнянні з прямим циліндром. Для тіл, виконаних із функціонально-градієнтного матеріалу, вплив вирізу на напружено-деформований стан менш виражено.

***Ключові слова**: функціонально-градієнтний матеріал, тіло обертання, повзучість, метод R-функцій.*

Література

1. Chen J. J. Creep analysis for a functionally graded cylinder subjected to internal and external pressure. *J. Strain Analysis*. 2007. Vol. 42. P 69–77. https://doi.org/10.1243/03093247JSA237
2. Nejad M. Z., Kashkoli M. D. Time-dependent thermo-creep analysis of rotating FGM thick-walled cylindrical pressure vessels under heat flux. *Int. J. Eng. Sci.* 2014. Vol. 82. P. 222–237. https://doi.org/10.1016/j.ijengsci.2014.06.006.
3. Shrikant K. V. Creep analysis of an isotropic functionally graded cylinder. *J. Advances in Sci. and Techn.* 2012. Vol. 3. No. 4. P. 1–9.
4. Singh T., Gupta V. K. Effect of anisotropy on steady state creep in functionally graded cylinder. *Composite Structures.* 2011. Vol. 93. No. 2. P. 747–758. https://doi.org/10.1016/j.compstruct.2010.08.005.
5. Chen J. J., Yoon K. B., Tu S. T. Creep behavior of pressurized tank composed of functionally graded materials. *J. Pressure Vessel Techn.* 2011. Vol. 133. P. 69–77. https://doi.org/10.1115/1.4003455.
6. Kashkoli M. D., Nejad M. Z. Time dependent thermo-elastic creep analysis of thick-walled spherical pressure vessels made of functionally graded materials. *J. Theoret. and Appl. Mech.* 2015. Vol. 53. No. 4. P. 1053–1065. https://doi.org/10.15632/jtam-pl.53.4.1053.
7. Бреславський Д. В., Коритко Ю. М., Татарінова О. А. Проектування та розробка скінченноелементного програмного забезпечення. Харків: «Підручник НТУ «ХПІ», 2017. 232 с.
8. Breslavsky D., Kozlyuk A., Tatatarinova O. Numerical simulation of two-dimensional problems of creep crack growth with material damage consideration. *Eastern-European Journal of Enterprise Technologies.* 2018. No. 2/7 (92). P. 27–33. https://doi.org/10.15587/1729-4061.2018.119727.
9. Рвачев В. Л. Теория R-функций и некоторые ее приложения. Киев: Наук. думка, 1982. 552 с.
10. Рвачев В. Л., Синекоп Н. С. Метод R-функций в задачах теории упругости и пластичности. Киев: Наук. думка, 1990. 216 с.
11. Rodichev Y. M., Smetankina N. V., Shupikov O. M., Ugrimov S. V. Stress-strain assessment for laminated aircraft cockpit windows at static and dynamic loads. *Strength of Materials*. 2018. Vol. 50. Iss. 6. P. 868–873. https://doi.org/10.1007/s11223-019-00033-4.
12. Сметанкіна Н. В. Моделювання коливань шаруватих циліндричних оболонок складної форми при ударному навантаженні. *Вісн. Запоріз. нац. ун-ту. Фізико-математичні науки*. 2015. № 1. С. 162–170.
13. Zolochevsky A., Sklepus S., Galishin A., Kühhorn A., Kober M. A comparison between the 3D and the Kirchhoff-Love solutions for cylinders under creep-damage conditions. *Techn. Mechanik*. 2014. Vol. 34**.** No. 2. P. 104–113.
14. Singh S. B., Ray S. Creep analysis in an isotropic FGM rotating disc of Al–SiC composite. *J. Materials Proc. Techn.* 2003. Vol. 143–144. P. 616-622. https://doi.org/10.1016/S0924-0136(03)00445-X.
15. Ogierman W., Kokot G. Mean field homogenization in multi-scale modelling of composite materials. *J. Achievements in Materials Manufacturing Eng. (JAMME)*. 2013. Vol. 61. Iss. 2. P. 343–348.
16. Singla A., Gard M., Gupta V. K. Steady state creep behaviour of functionally graded composite by using analytical method. *Intern. J. Computer Appl.* 2015. No. 8. P. 13–17.